Supporting Information

Ligand Dependence of Binding to Three-Coordinate

Fe(II) Complexes

Karen P. Chiang, Pamela M. Barrett, Feizhi Ding, Jeremy M. Smith, Savariraj Kingsley, William W.

Brennessel, Meghan M. Clark, Rene J. Lachicotte, Patrick L. Holland*

Figure S1. ORTEP drawing of the molecular structure of $L^{tBu,iPr2}Fe(SPh)$. Thermal ellipsoids at 50% probability. Hydrogen atoms omitted for clarity.
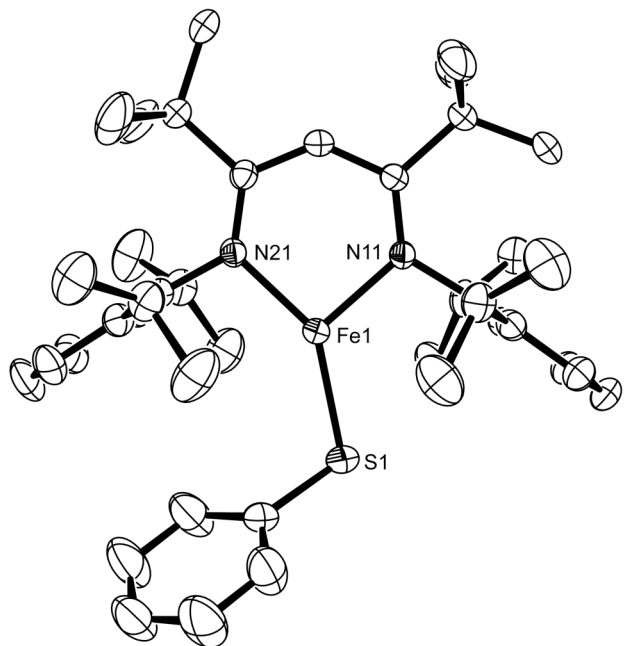

Figure S2. ORTEP drawing of the molecular structure of $L^{tBu,iPr2}Fe(SPhCF_3)$. Thermal ellipsoids at 50% probability. Hydrogen atoms omitted for clarity.
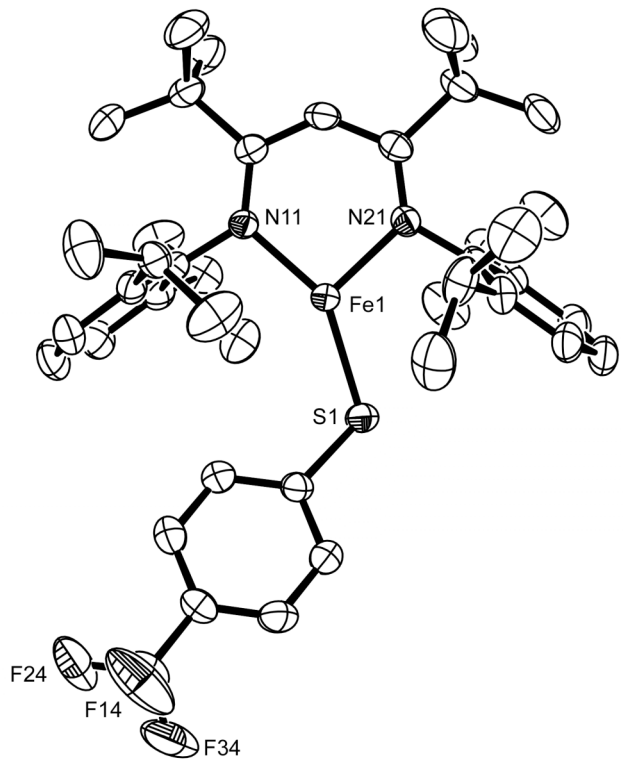
Figure S3. UV-Vis plot of L^{tBu,iPr2}FeCl with specified amount of DMF. Values in the key correspond to the concentration of DMF in that sample. The concentration of L^{tBu,iPr2}FeCl was 1 mM for each sample.
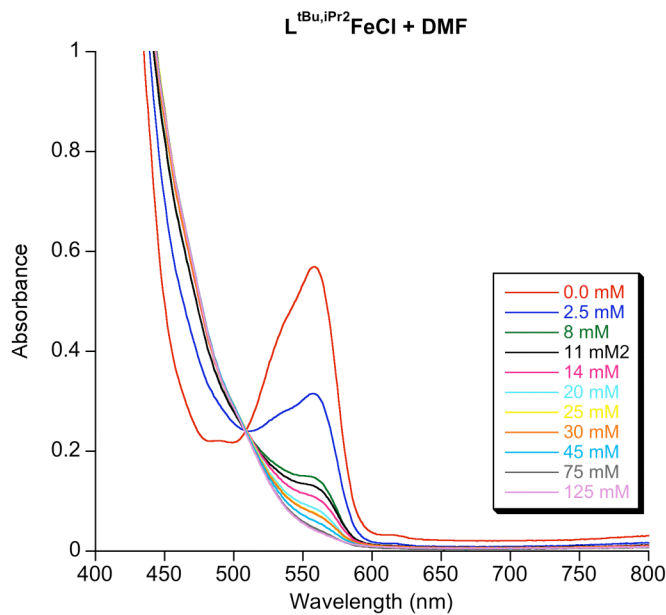

Figure S4. UV-Vis plot of L^{tBu,iPr2}FeCl with specified amount of 2-Picoline. The concentration of L^{tBu,iPr2}FeCl was 1 mM for each sample.
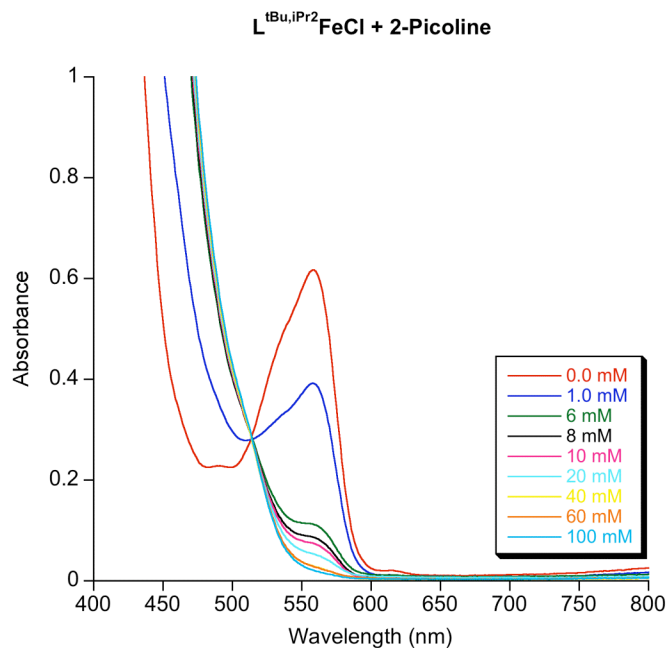
Figure S5. UV-Vis plot of $L^{tBu,iPr2}Fe(SPh)$ with specified amount of CN^tBu. The concentration of $L^{tBu,iPr2}Fe(SPh)$ was 1 mM for each sample.

$$L^{tBu,iPr2}Fe(SPh) + CN^tBu$$
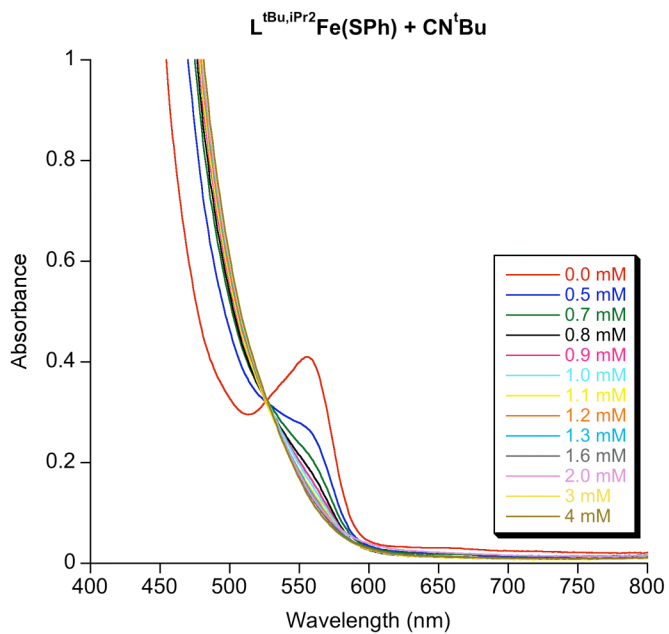
Figure S6. Binding curve of $L^{tBu,iPr2}FeCl$ and PPh_3 in toluene. $K_{eq} = 0.7 \pm 0.08$.
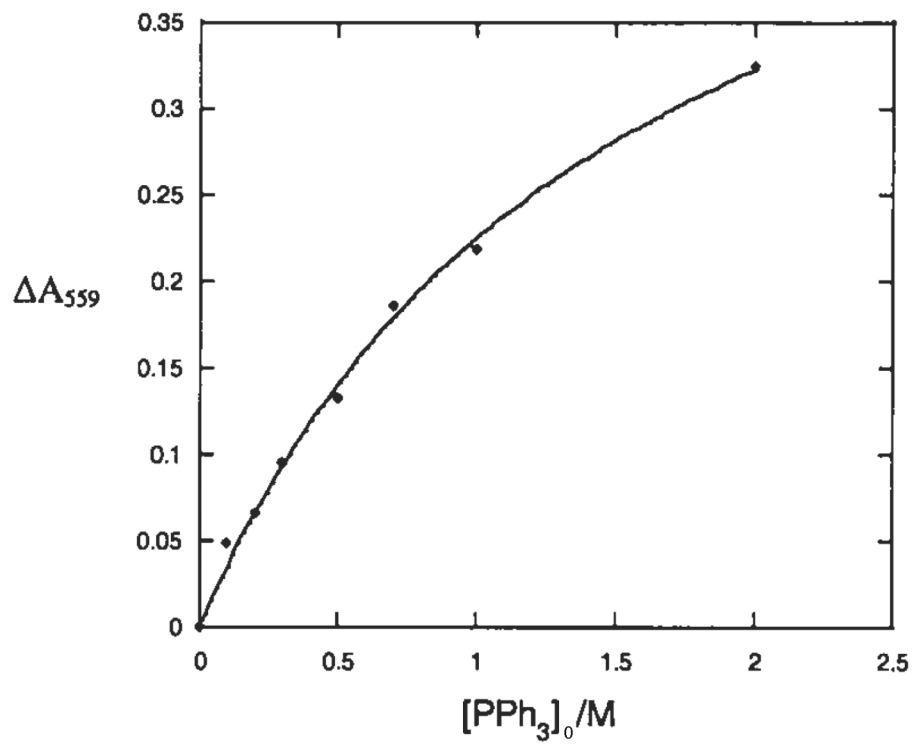
Figure S7. Binding curve of $L^{tBu,iPr2}FeCl$ and THF in toluene. $K_{eq} = 0.8 \pm 0.01$
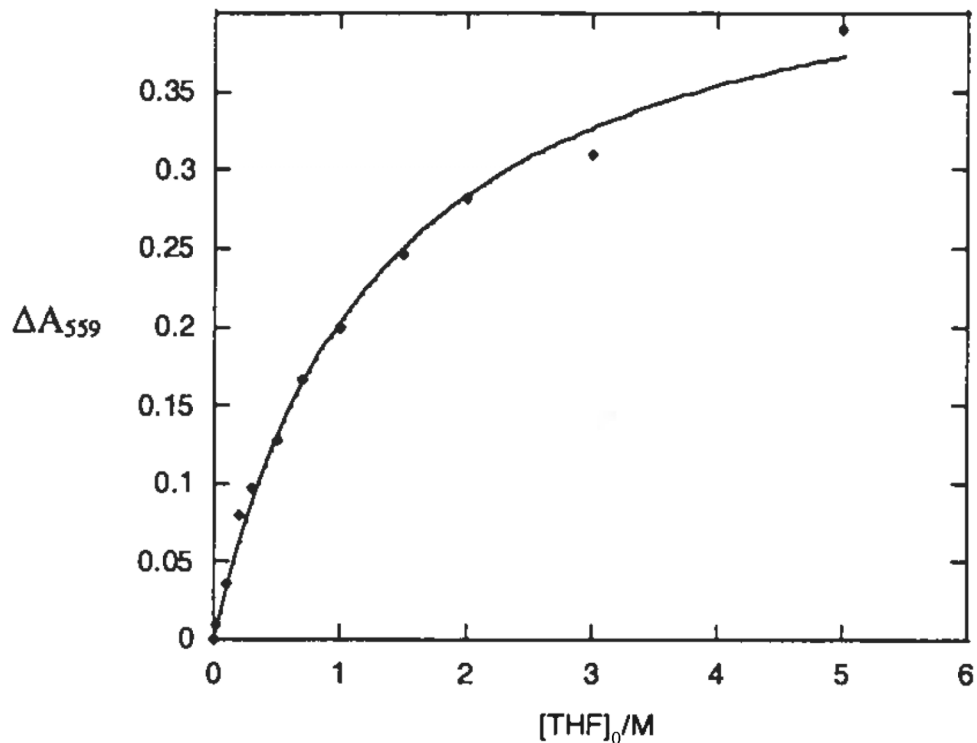
Figure S8. Binding curve of $L^{tBu,iPr2}FeCl$ and MeCN in toluene. $K_{eq} = 9.8 \pm 0.5$
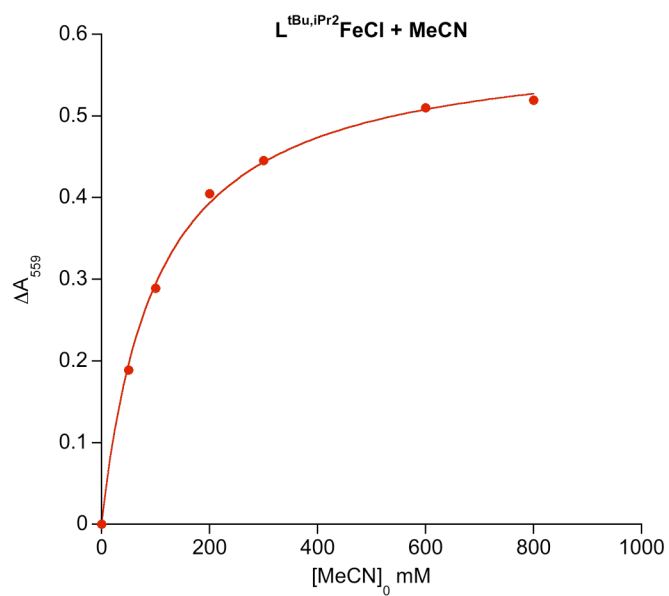
Figure S9. Binding curve of $L^{tBu,iPr2}FeCl$ and DMF in toluene. $K_{eq} = 390 \pm 20$
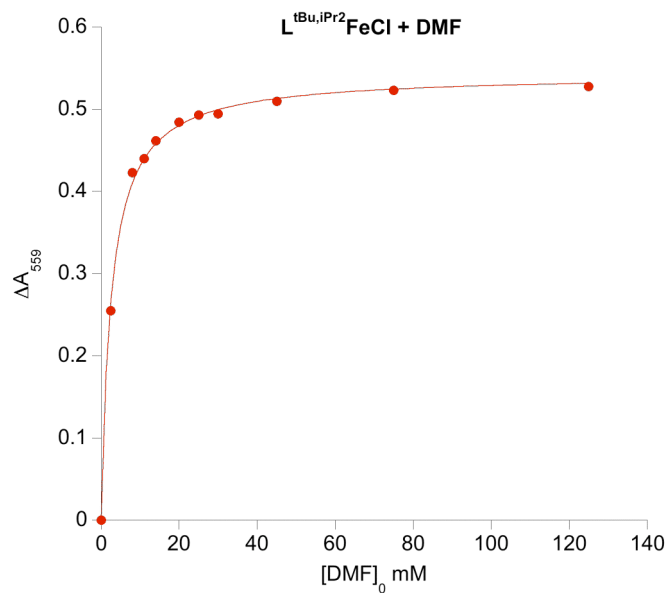
Figure S10. Binding curve of $L^{tBu,iPr2}FeCl$ and 2-picoline in toluene. $K_{eq} = 660 \pm 50$
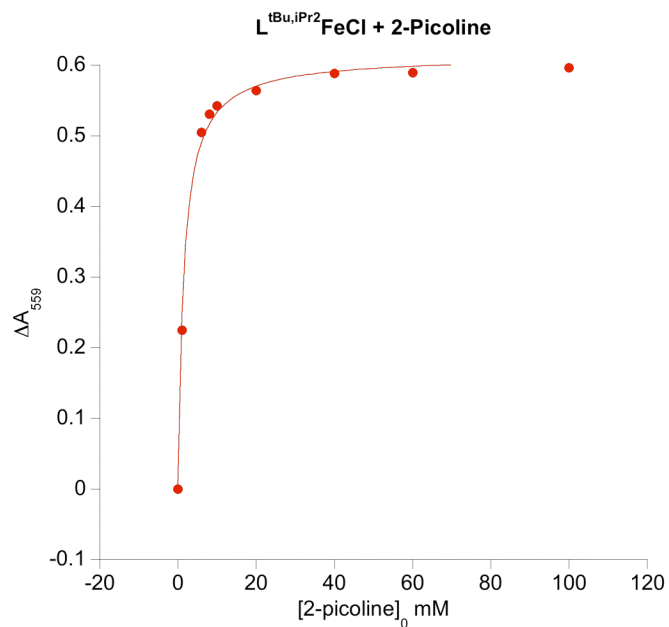
Figure S11. Binding curve of $L^{tBu,iPr2}$FeCl and pyridine in toluene. $K_{eq} = 41000 \pm 6000$
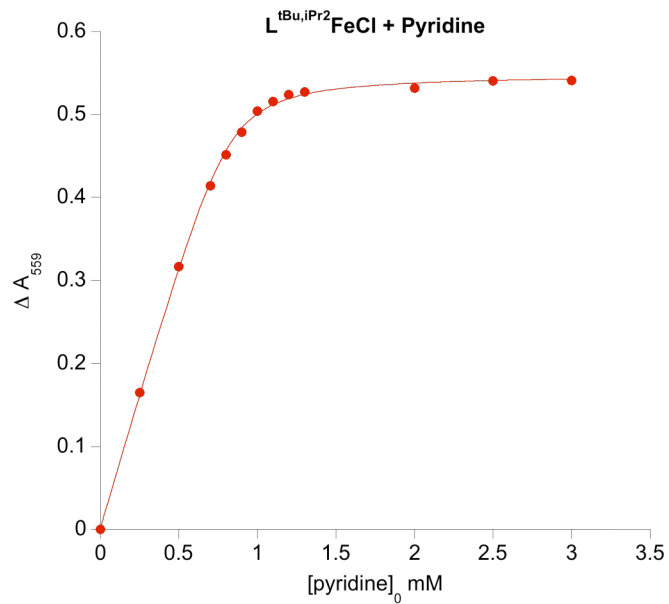
Figure S12. Binding curve of $L^{tBu,iPr2}$FeCl and $CN^{t}Bu$ in toluene. $K_{eq} = 73000 \pm 27000$
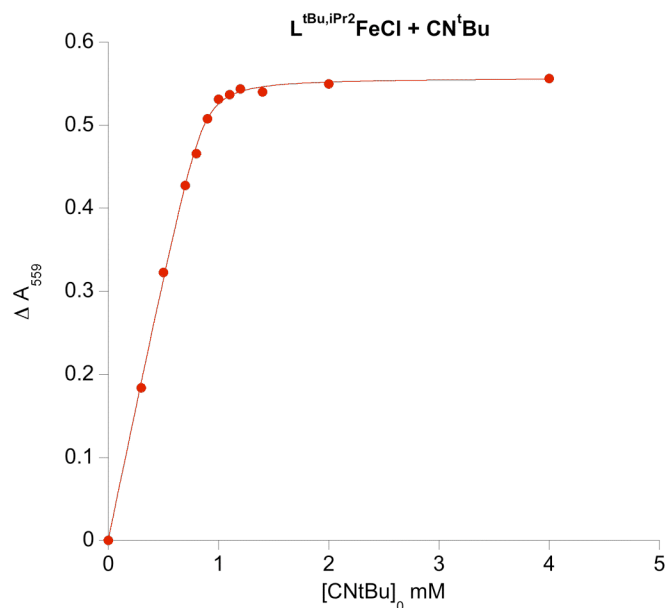
Figure S13. Binding curve of $L^{tBu,iPr2}FeSPh$ and PPh_3 in toluene. $K_{eq} = 1.0 \pm 0.5$
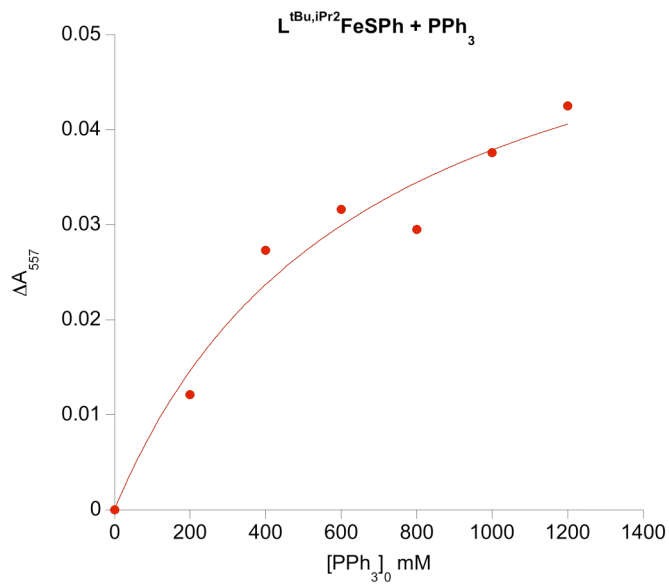
**Figure S14.** Binding curve of $L^{tBu,iPr2}FeSPh$ and THF in toluene. $K_{eq} = 0.15 \pm 0.01$
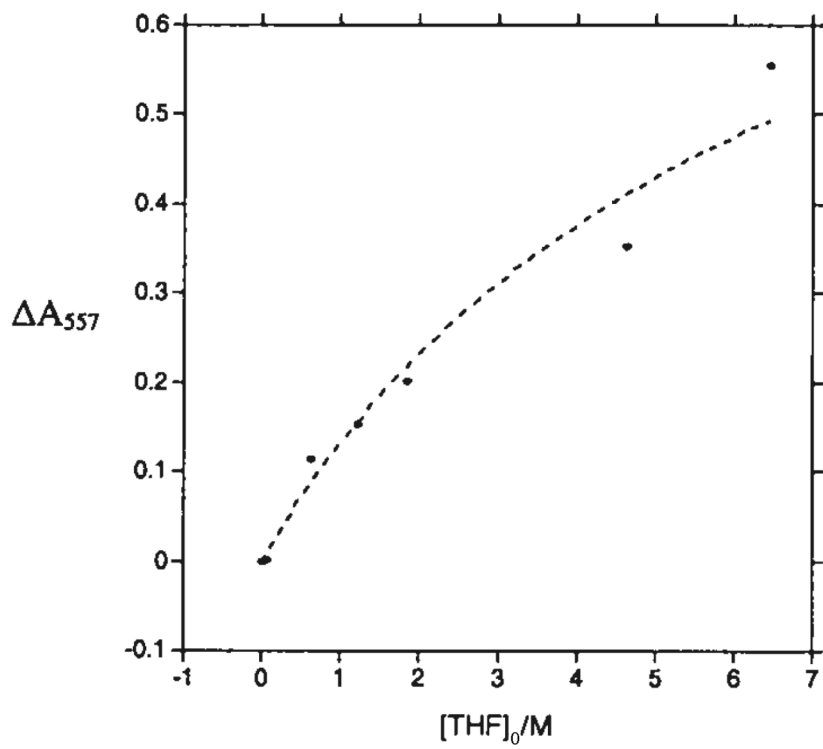
**Figure S15.** Binding curve of $L^{tBu,iPr2}$FeSPh and MeCN in toluene. $K_{eq} = 5.2 \pm 0.2$
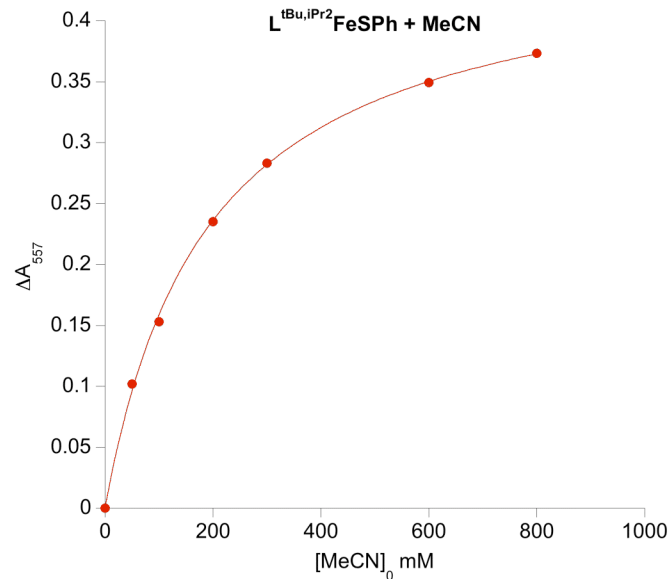
Figure S16. Binding curve of $L^{tBu,iPr2}$FeSPh and DMF in toluene. $K_{eq} = 160 \pm 5$
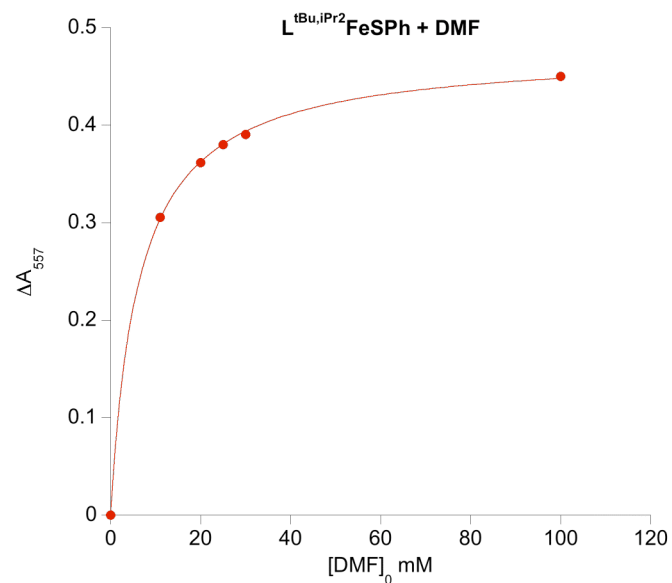
Figure S17. Binding curve of $L^{tBu,iPr2}$FeSPh and 2-picoline in toluene. $K_{eq} = 300 \pm 30$

$L^{tBu,iPr2}$FeSPh + 2-picoline
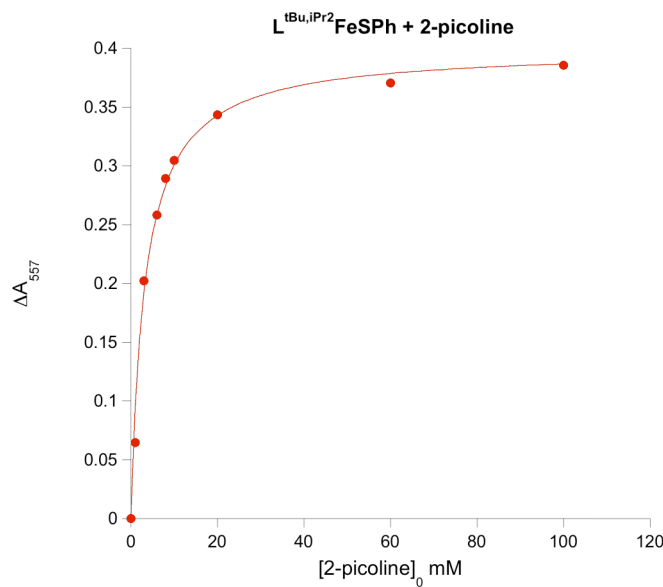
Figure S18. Binding curve of $L^{tBu,iPr2}$FeSPh and pyridine in toluene. $K_{eq} = 11000 \pm 2000$

$L^{tBu,iPr2}$FeSPh + Pyridine
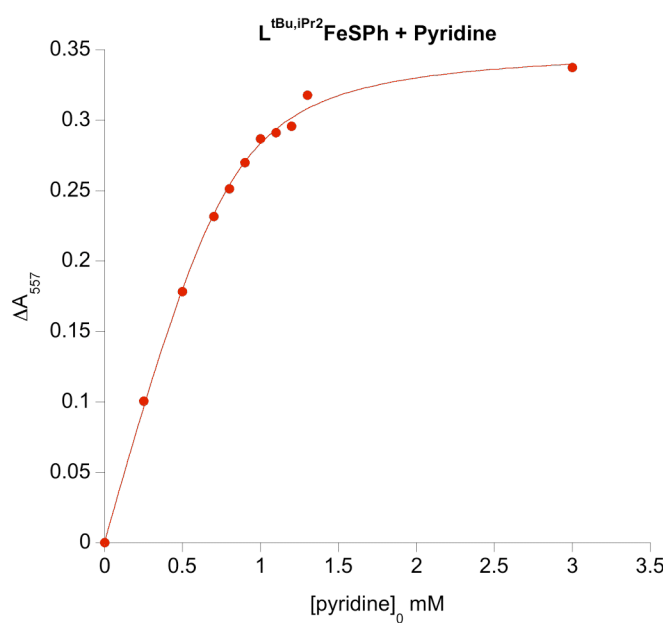
Figure S19. Binding curve of $L^{tBu,iPr2}Fe(SPhCF_3)$ and MeCN in toluene. $K_{eq} = 11.7 \pm 0.9$
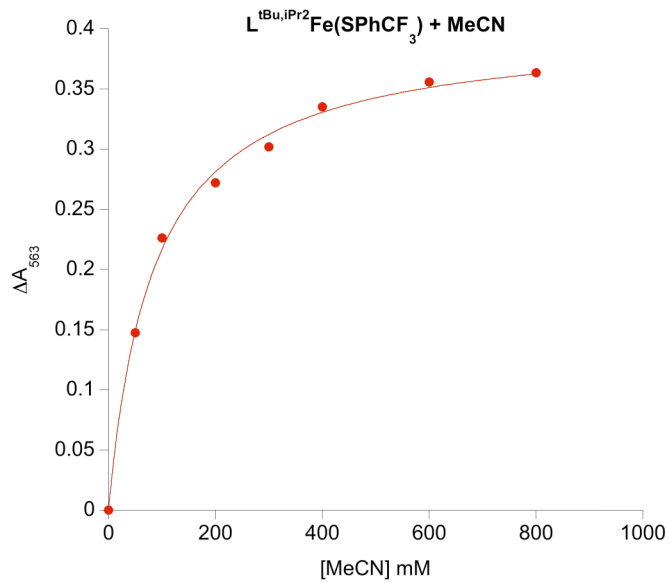
Figure S20. Binding curve of $L^{tBu,iPr2}Fe(SPhCF_3)$ and DMF in toluene. $K_{eq} = 230 \pm 10$
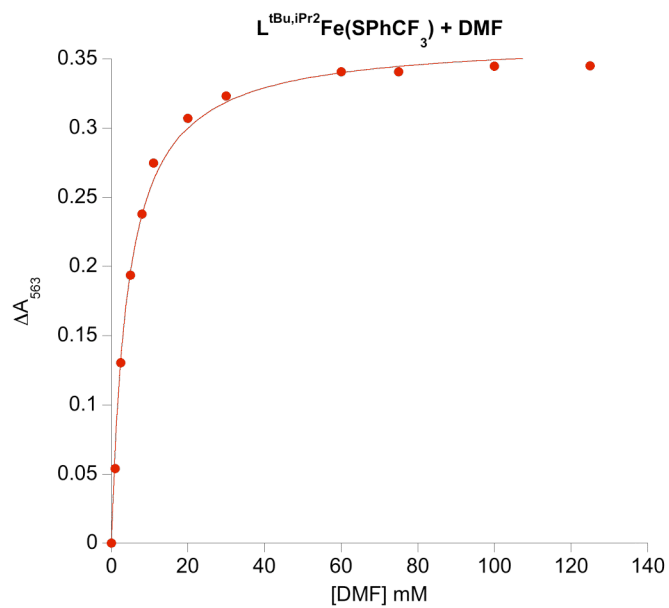
Figure S21. Binding curve of $L^{tBu,iPr2}Fe(OPh)$ and MeCN in toluene. $K_{eq} = 4.7 \pm 0.4$
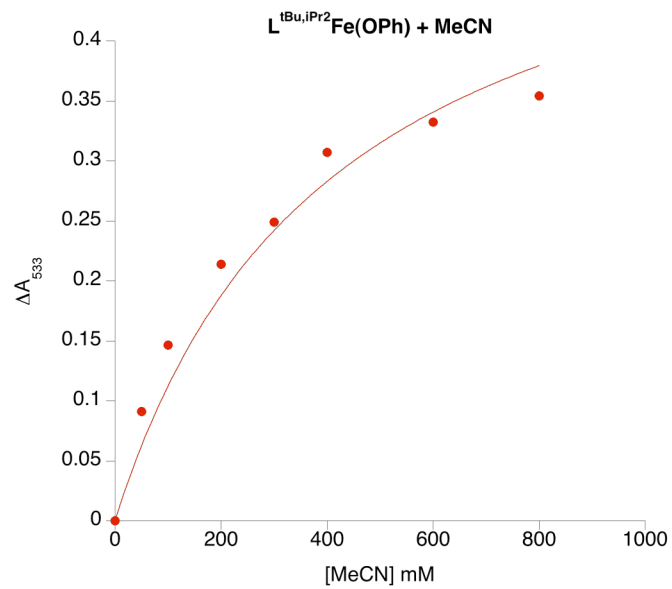
**Figure S22.** Binding curve of $L^{tBu,iPr2}Fe(OPh)$ and DMF in toluene. $K_{eq} = 160 \pm 10$
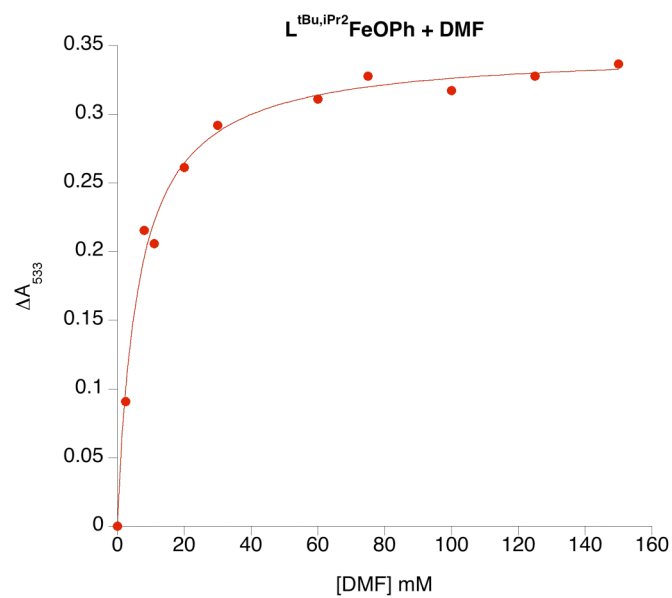
Figure S23. Voltammogram of $L^{tBu,iPr2}Fe(SPh)$ with corresponding $E_{1/2}$ value of -2.41(2) V. Potential is referenced to the Fc^+/Fc couple. The sample consisted of 4 mM of $L^{tBu,iPr2}Fe(SPh)$ in Et_2O with 0.1 M NBu_4BArF.
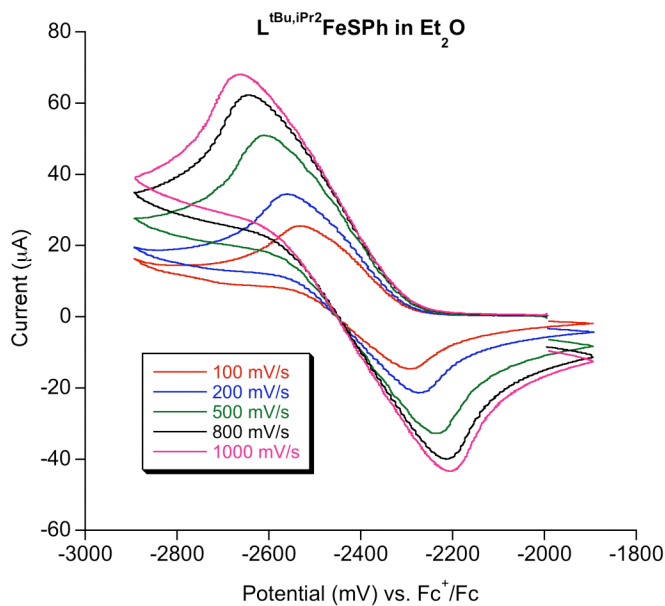
Figure S24. Voltammogram of $L^{tBu,iPr2}Fe(SPhCF_3)$ with corresponding $E_{1/2}$ value of -2.40(2) V. Potential is referenced to the Fc^+/Fc couple. The sample consisted of 4 mM of $L^{tBu,iPr2}Fe(SPhCF_3)$ in Et_2O with 0.1 M NBu_4BArF.
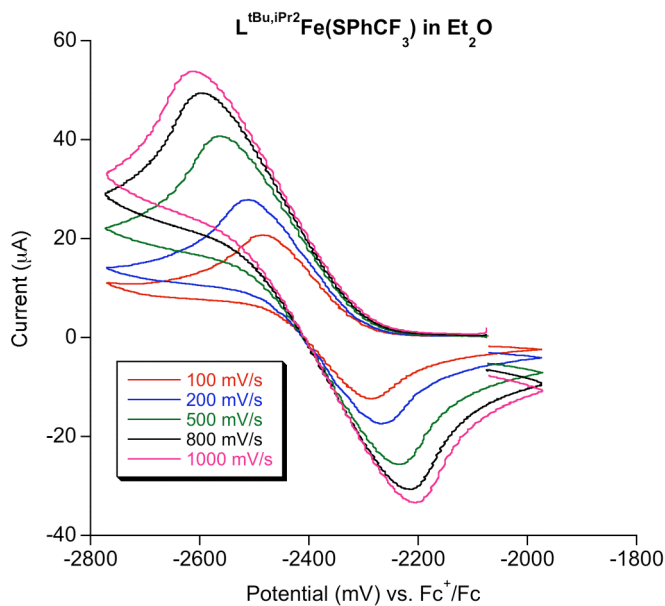
Figure S25. Voltammogram of $L^{tBu,iPr2}Fe(OPh)$ with corresponding $E_{1/2}$ value of -2.56(3) V. Potential is referenced to the Fc^+/Fc couple. The sample consisted of 4 mM of $L^{tBu,iPr2}Fe(OPh)$ in Et_2O with 0.1 M NBu_4BArF.
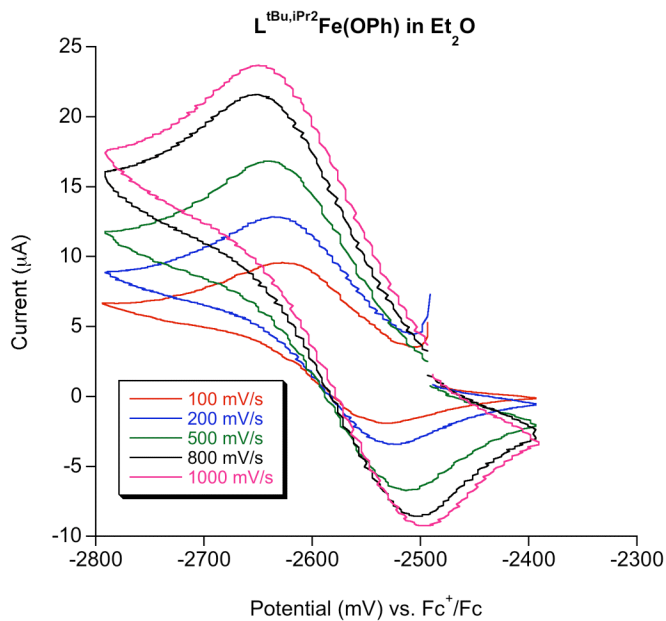
Figure S26 CV of $L^{tBu,iPr2}FeCl$ sweeping in the reduction (left) and oxidation (right) direction. The reduction peak at -320 mV is correlated with the oxidation peak at 430 mV. Potentials are referenced to the Fc^+/Fc couple.
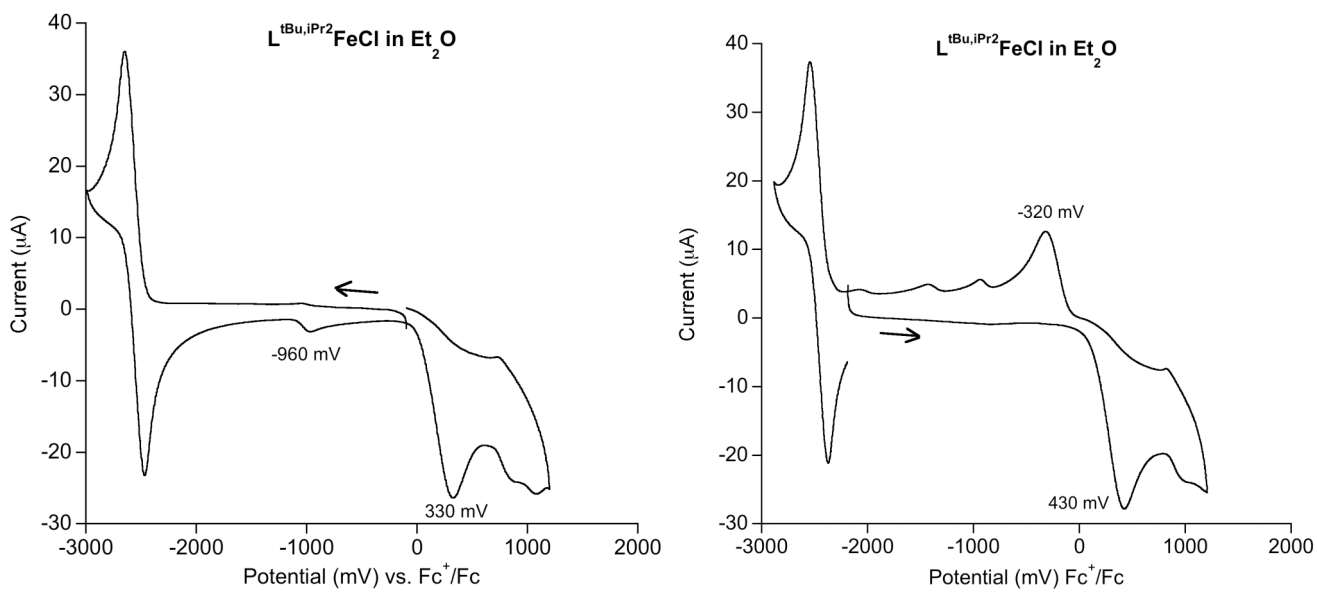
Figure S27. Voltammogram of $L^{tBu,iPr2}Fe(SPh)(NCMe)$ with corresponding $E_{1/2}$ value of -2.30(6) V. Potential is referenced to the Fc^+/Fc couple. The sample consisted of 4 mM of $L^{tBu,iPr2}Fe(SPh)$ in MeCN with 0.1 M NBu_4PF_6.
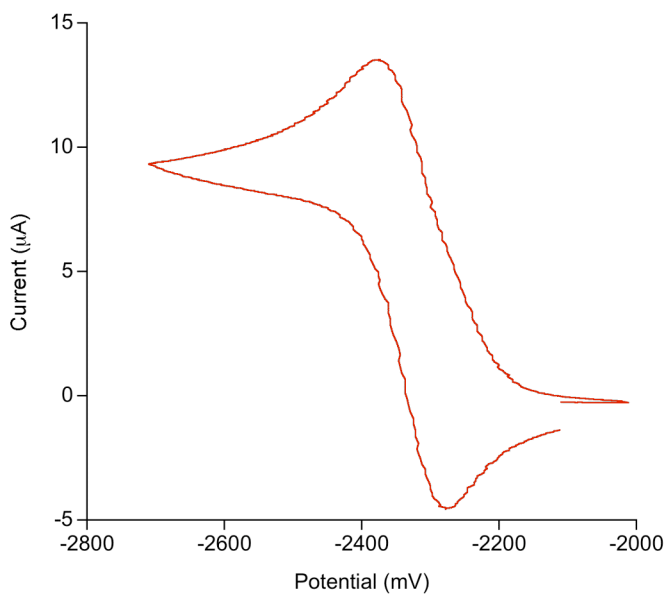
Figure S28. Voltammogram of $L^{tBu,iPr2}Fe(SPhCF_3)(NCMe)$ with corresponding $E_{1/2}$ value of -2.33(1) V. Potential is referenced to the Fc^+/Fc couple. The sample consisted of 4 mM of $L^{tBu,iPr2}Fe(SPhCF_3)$ in MeCN with 0.1 M NBu_4PF_6.

15
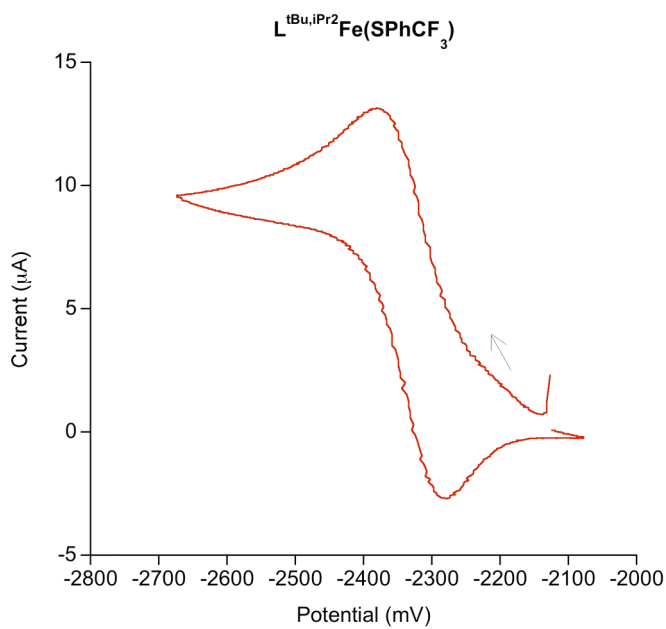
Figure S29. Voltammogram of $L^{tBu,iPr2}Fe(OPh)(NCMe)$ with corresponding $E_{1/2}$ value of -2.27(6) V. Potential is referenced to the Fc^+/Fc couple. The sample consisted of 4 mM of $L^{tBu,iPr2}Fe(OPh)$ in MeCN with 0.1 M NBu_4PF_6.
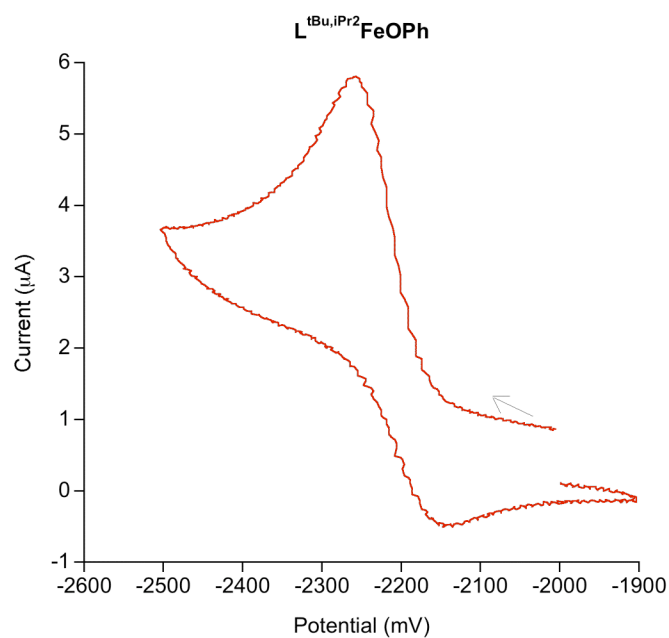
Figure S30. CV of $L^{tBu,iPr2}FeCl(NCMe)$ sweeping in the reduction direction first. Potentials are referenced to the Fc^+/Fc couple.
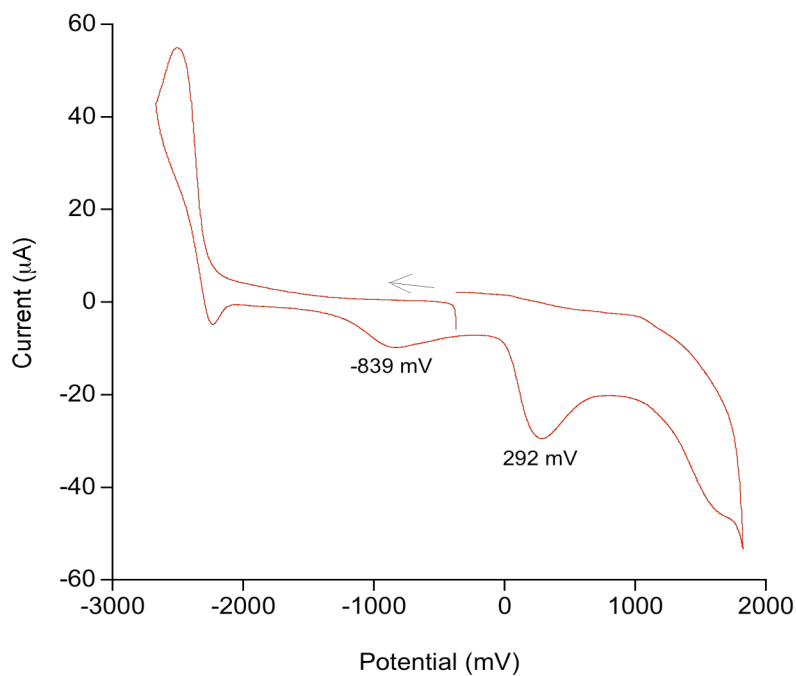
Figure S31. CV of L^{tBu,iPr2}FeCl(NCMe) sweeping in the oxidation direction first. An irreversible oxidation (E$_{pa}$ = 12(9) mV) as well as reduction (E$_{pc}$ = -67(3) mV) is observed. Potentials are referenced to the Fc$^+$/Fc couple.
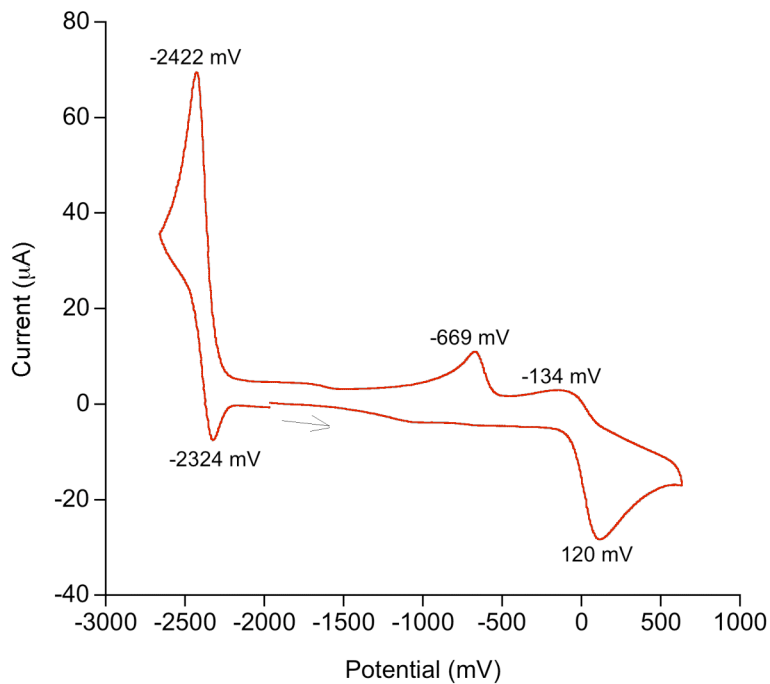
Figure S32. CV of the irreversible oxidation and reduction waves of L^{tBu,iPr2}FeCl(NCMe). Potentials are referenced to the Fc$^+$/Fc couple.
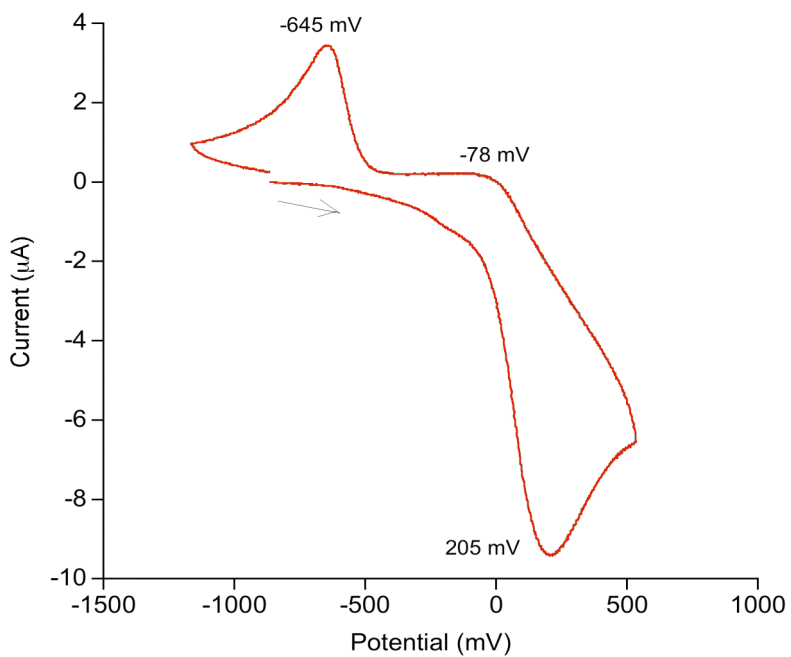
Table S1. List of compounds in the CSD used to determine solid and cone angles of PPh_3. The metal of the complex is iron unless otherwise noted. "Coord. #" denotes coordination number of the metal center.

	Ligand: PPh_3			
Coord. #	Compound	Solid Ang (Ω)	Cone Ang (θ)	P#
4-coord.	DPPNFE	3.35	124.34	1
	GATXOP	3.33	123.96	1
		3.33	123.96	1A
	GAWPUP	3.29	123.07	2
		3.39	125.27	3
	JUQDAA	3.41	125.53	1
	OJAPOE	3.42	125.77	4
6-coord.	CUBDOS	3.29	123.15	1
	DASFAF	3.19	120.94	1
	FEHBEA	3.31	123.15	2
	GACLOL	3.32	123.66	2
	REYFIL	3.29	123.18	1
		3.27	122.72	2
	YAWGUY	3.27	122.76	1
	YEMYAR	3.29	123.02	1
	Avg.	3.32	124	
	Std. Dev.	0.06	1	

Table S2. List of compounds in the CSD used to determine solid and cone angles of THF.

Coord. #	Compound	Solid Ang (Ω)	Cone Ang (θ)	O#
		Ligand: THF		
4-coord.	DABPUS	1.81	89.22	1
	DABQAZ	1.79	88.78	1
	GUWVUP	1.82	89.45	1
		1.82	89.41	1F
	JIXLEH	1.79	88.58	2
		1.79	88.57	2B
	MEZBOI	1.83	89.72	3
		1.80	89.02	4
	VEMYOB	1.78	88.54	1
	WORPIC	1.67	85.58	1
		1.67	85.58	1A
	YECRII	1.80	88.98	1
		1.79	88.60	2
	YECRUU	1.81	89.30	1
		1.79	88.76	2
5-coord.	CIZFEWO1	1.87	91.66	1
		1.92	92.13	2
		1.81	89.27	3
		1.87	90.66	1A
		1.92	92.12	2A
		1.81	89.27	3A
	KAJTOE	1.88	91.05	1
		1.80	91.03	1E
	Avg.	1.81	89	
	Std. Dev.	0.06	2	

Table S3. List of compounds in the CSD used to determine solid and cone angles of MeCN.

Coord. #	Compound	Solid Ang (Ω)	Cone Ang (θ)	N#
		Ligand: MeCN		
4-coord.	DABRII	1.60	83.68	4
	JEWTUB	1.60	83.68	5
		1.60	83.74	6
	LEJQUN	1.60	83.73	1
	LUGNOQ	1.60	83.75	1
		1.60	83.68	2
	NASKEY	1.60	83.68	3
5-coord.	MAKCAD	1.60	83.74	3
	YEPDUS	1.60	83.64	11
	OFACEE	1.60	83.71	3
6-coord.	AVINUO	1.60	83.63	6
	EBORIW	1.60	83.71	5
		1.60	83.67	6
	ESUQOY	1.60	83.69	5
		1.60	83.66	6
	IROHOM	1.60	83.72	6
		1.60	83.67	12
	NELGUG	1.60	83.66	5
		1.60	83.66	6
	RIYTIC	1.60	83.68	5
		1.60	83.65	6
	Avg.	1.60	83.69	
	Std. Dev.	0.00	0.03	

Table S4. List of compounds in the CSD used to determine solid and cone angles of DMF. Holkc01 is L^{tBu,iPr2}Fe(SPh)(DMF) (Figure 4c) reported in this paper. We used the ten complexes in the CSD with Fe-O-C and O-C-N angles closest to those in L^{tBu,iPr2}Fe(SPh)(DMF). The differences in angles from complexes in the database are shown; variations up to 14° did not affect the accuracy of the solid and cone angles (small standard deviation).

Coord. #	Compound	Fe-O-C (°)	Δ Fe-O-C (°)	O-C-N (°)	Δ O-C-N (°)	Solid Ang (Ω)	Cone Ang (θ)	O#
4-coord.	**HOLKC01**	**118.21**	**0**	**124.84**	**0**	**1.69**	**86.18**	**15**
5-coord.	JIWMIL	126.295	8.085	123.916	0.924	1.62	84.15	4
	QEKXIO	124.604	6.394	124.375	0.465	1.63	84.46	1
	GIGGIN	124.814	6.604	124.943	0.103	1.62	84.30	1
6-coord.	DEZMIF	127.752	9.542	126.414	1.574	1.60	83.49	1
		122.61	4.4	123.841	0.999	1.64	84.68	2
		124.329	6.119	125.643	0.803	1.63	84.36	3
	GAZGET	118.366	0.156	125.493	0.653	1.71	86.55	1
		123.371	5.161	128.987	4.147	1.67	85.49	4
		127.452	9.242	128.674	3.834	1.63	84.37	2
		121.441	3.231	127.51	2.67	1.68	85.91	5
		132.071	13.861	121.519	3.321	1.58	83.05	3
		129.566	11.356	125.658	0.818	1.60	83.69	6
	JOHVIL	127.944	9.734	123.629	1.211	1.61	83.92	9
		123.173	4.963	120.805	4.035	1.64	84.73	10
	LOXYIG	116.953	1.257	125.936	1.096	1.70	86.26	1
	NADTAN	132.766	14.556	123.065	1.775	1.56	82.65	1
		126.309	8.099	124.523	0.317	1.62	84.05	1
		132.732	14.522	122.211	2.629	1.57	82.67	1
		125.518	7.308	124.144	0.696	1.63	84.33	1
		124.739	6.529	124.045	0.795	1.63	84.43	1
	QEZGUY	129.333	11.123	123.66	1.18	1.59	83.40	1
		125.262	7.052	124.655	0.185	1.63	84.33	2
	WODKIJ	117.23	0.98	124.455	0.385	1.67	85.57	6
	CIDLUX	126.042	7.832	125.534	0.694	1.61	84.03	10
		129.682	11.472	122.443	2.397	1.58	83.17	11
	MIJKOG	128.207	9.997	129.494	4.654	1.60	83.74	18
		123.958	5.748	129.279	4.439	1.64	84.70	19
		121.468	3.258	127.766	2.926	1.60	85.21	14
		131.329	13.119	133.167	8.327	1.74	87.28	15
		121.969	3.759	126.884	2.044	1.70	86.38	16
					Avg.	1.63	85	
					Std. Dev.	0.04	1	

21

Table S5. List of compounds in the CSD used to determine solid and cone angles of 2-picoline. Only two compounds with 2-picoline as a ligand were found. Therefore, cobalt and nickel complexes were also used to calculate the solid and cone angle of 2-picoline.

Ligand: 2-Picoline

Coord. #	Compound	Solid Ang (Ω)	Cone Ang (θ)	N#
Fe, 6-Coord	OMAJUH	2.39	103.44	1
		2.39	103.43	1A
	QANNAU	2.33	102.10	1
		2.37	102.96	2
		2.36	102.66	3
		2.34	102.37	4
Co, 4-Coord	WUGTOH	2.40	103.67	2
Ni, 6-Coord	KUHBOE	2.34	102.22	1
		2.34	102.24	1A
	Avg.	2.36	102.8	
	Std. Dev.	0.03	0.6	

Table S6. List of compounds in the CSD used to determine solid and cone angles of pyridine.

Ligand: Pyridine

Coord. #	Compound	Solid Ang (Ω)	Cone Ang (θ)	N#
4-Coord.	DAWKAO	1.89	91.39	1
		1.89	91.36	2
	HEVLAW	1.89	91.23	1
	KAHJUZ	1.89	91.39	3
		1.89	91.36	4
	MEGHUC	1.90	91.60	3
	POMZOG	1.94	92.53	1
		1.95	92.85	2
	QANMOH	1.90	91.43	1
		1.89	91.40	2
	TENHOJ	1.90	91.43	1
		1.90	91.43	1B
5-Coord.	QEVCEA	1.90	91.53	1
	RORKUE	1.92	92.03	5
	SELSEI	1.89	91.36	7
	Avg.	1.90	91.6	
	Std.Dev.	0.02	0.5	

Table S7. List of compounds in the CSD used to determine solid and cone angles of CN^{t}Bu. Holkc02 is L^{tBu,iPr2}Fe(SPh)(CN^{t}Bu) (Figure 4a) reported in this paper. We used the ten complexes in the CSD with Fe-C-N and C-N-C angles closest to those in L^{tBu,iPr2}Fe(SPh)(CN^{t}Bu). The differences in angles from complexes in the database are shown; variations up to 12° did not affect the accuracy of the solid and cone angles (small standard deviation).

<div align="center">

Ligand: CN^{t}Bu

</div>

Coord. #	Compound	Fe-C-N (°)	Δ Fe-C-N (°)	C-N-C (°)	Δ C-N-C (°)	Solid Ang (Ω)	Cone Ang (θ)	C#
	HOLKC02	**165.46**	**0**	**173.58**	**0**	**1.66**	**85.30**	C15
4-coord.	WAHGIV	174.576	9.116	165.018	8.562	1.65	84.92	C21
		177.268	11.808	176.33	2.75	1.65	84.89	C26
	YACJIW	168.668	3.208	176.856	3.276	1.65	84.95	C27
		168.879	3.419	173.124	0.456	1.65	84.92	C21
5-coord.	PUSYAD	172.582	7.122	163.945	9.635	1.65	85.06	C1
		173.147	7.687	165.925	7.655	1.65	84.91	C2
		176.203	10.743	173.422	0.158	1.65	84.89	C3
		175.944	10.484	168.234	5.346	1.65	84.94	C6
		175.981	10.521	168.843	4.737	1.65	84.89	C5
	SIMVEP	177.266	11.806	164.159	9.421	1.65	84.98	C1
		171.762	6.302	165.729	7.851	1.65	84.91	C6
		173.674	8.214	163.326	10.254	1.65	84.91	C11
6-coord.	ENIXEE	173.852	8.392	176.222	2.642	1.65	84.93	C15
		174.763	9.303	177.233	3.653	1.65	84.98	C23
		172.943	7.483	177.484	3.904	1.65	84.94	C31
		176.645	11.185	172.789	0.791	1.65	84.94	C36
	FAJLAE	169.91	4.45	162.023	11.557	1.69	86.14	C36
		174.124	8.664	174.126	0.546	1.65	84.95	C84
		166.334	0.874	166.585	6.995	1.69	86.00	C44
		168.263	2.803	166.328	7.252	1.68	85.81	C89
	GOTFIE	177.651	12.191	172.737	0.843	1.65	84.89	C3
	KEWNIK	177.711	12.251	177.333	3.753	1.65	84.91	C1
		179.449	13.989	174.898	1.318	1.65	84.88	C10
		175.959	10.499	172.97	0.61	1.65	84.92	C15
		176.92	11.46	174.407	0.827	1.65	84.92	C20
	PAKKOC	167.539	2.079	167.922	5.658	1.65	84.96	C27
		171.938	6.478	175.371	1.791	1.66	85.25	C32
	QATRAE	171.539	6.079	169.462	4.118	1.66	84.96	C17
	VUPFAN	173.815	8.355	176.193	2.613	1.65	84.94	C23
		176.409	10.949	178.162	4.582	1.65	84.90	C28
	WAHBOW	172.343	6.883	173.252	0.328	1.65	84.93	C20
		170.714	5.254	170.544	3.036	1.65	85.04	C25

		171.616	6.156	166.735	6.845	1.65	85.08	C30
		174.971	9.511	167.214	6.366	1.65	84.89	C54
		174.399	8.939	174.135	0.555	1.65	84.89	C59
		177.04	11.58	167.737	5.843	1.65	84.85	C64
	YELVOA	177.343	11.883	167.803	5.777	1.65	84.95	C1
		175.084	9.624	173.46	0.12	1.65	84.98	C3
		174.383	8.923	162.99	10.59	1.65	84.88	C5
		178.516	13.056	164.124	9.456	1.65	84.92	C6
	YIBLUR	178.49	13.03	171.886	1.694	1.65	84.89	C5
		177.257	11.797	176.064	2.484	1.65	85.00	C13
					Avg.	1.65	85.0	
					Std. Dev.	0.01	0.3	

Figure S12. ^{1}H NMR spectrum of L^{tBu,iPr2}Fe(SPh)(CN^{t}Bu) in C$_6$D$_6$.
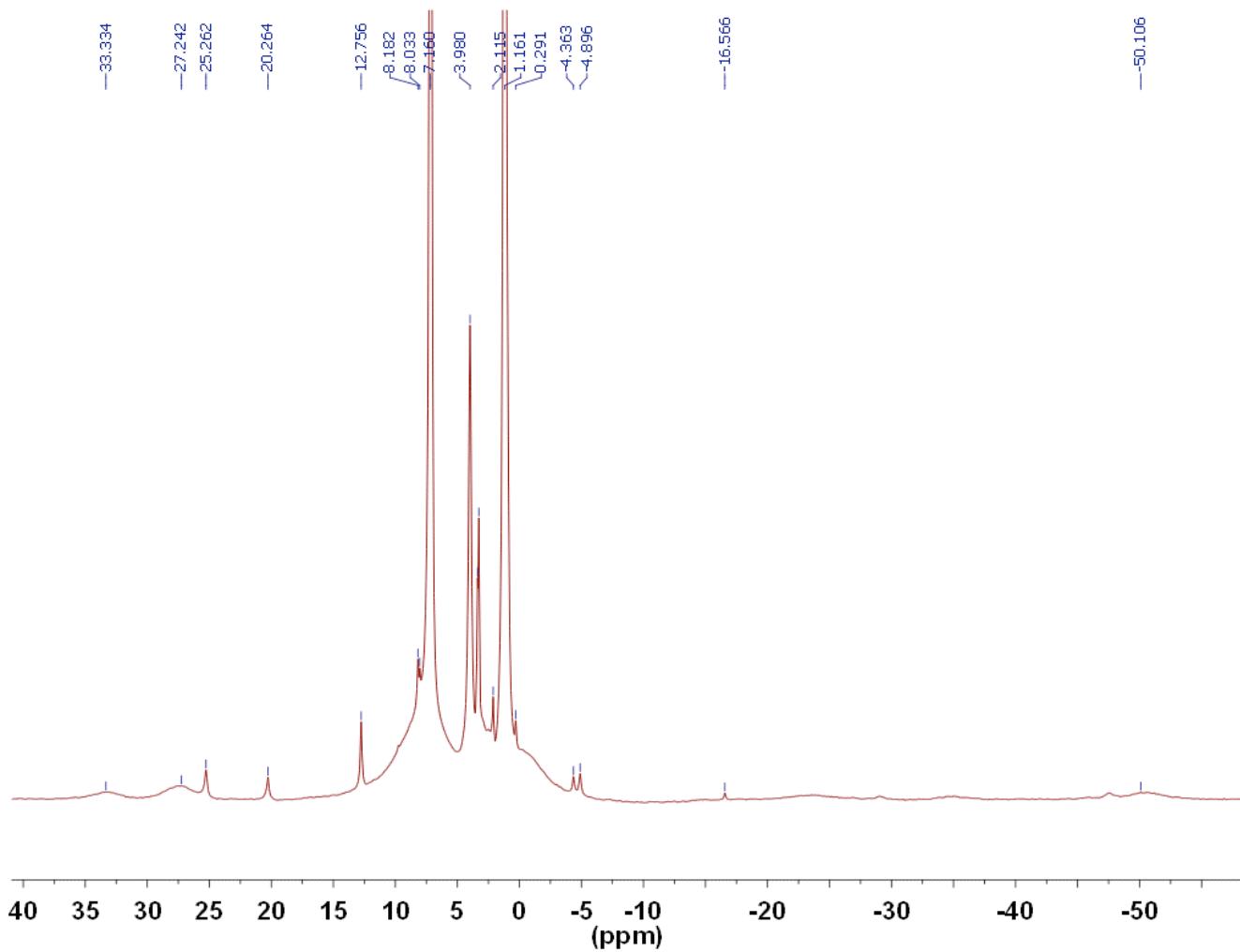
Figure S13. ^{1}H NMR spectrum of L^{tBu,iPr2}Fe(SPh)(DMF) in C$_6$D$_6$.
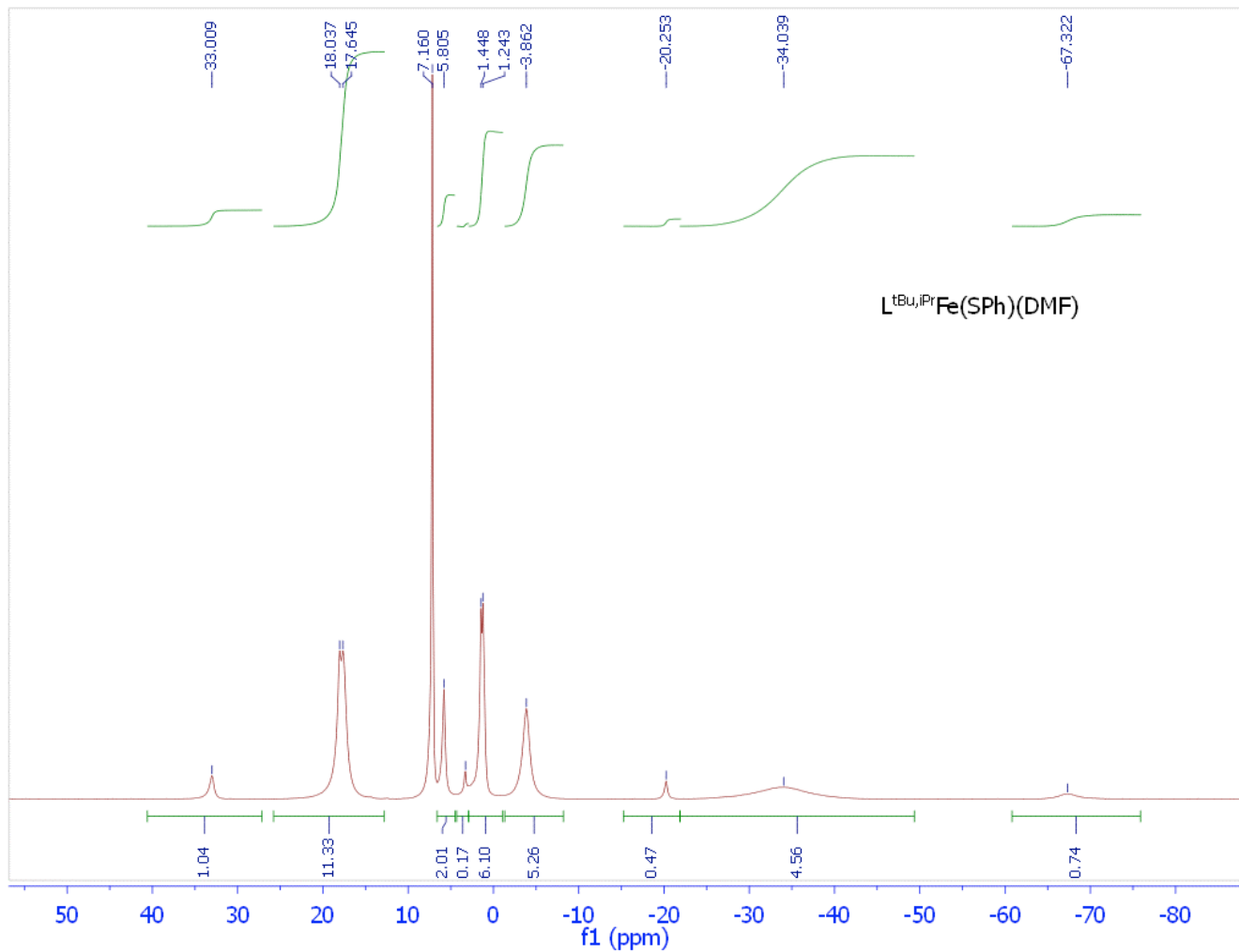
Figure S14. ^{1}H NMR spectrum of L^{tBu,iPr2}Fe(SPh)(MeIm) in C$_6$D$_6$.